

Effect of Molecular Structure of Hybrid Precursors on the Performances of Novel Hybrid Zwitterionic Membranes

Junsheng Liu,^{1,2} Tongwen Xu,¹ Guangneng Fan,² Yanxun Fu¹

¹Laboratory of Functional Membranes, School of Chemistry and Material Science, University of Science and Technology of China (USTC), Hefei 230026, China

²Department of Chemical and Materials Engineering, Hefei University, Hefei 230022, China

Received 11 December 2005; accepted 24 March 2006

DOI 10.1002/app.24486

Published online 11 May 2007 in Wiley InterScience (www.interscience.wiley.com).

ABSTRACT: Three types of novel hybrid zwitterionic membranes were prepared via a coupling reaction between two silane-coupling agents in a nonaqueous system and a subsequent reaction with 1,4-butyrolactone to create ion pairs in the hybrid precursors. FTIR spectra corroborated the corresponding reactions. The synthesized membranes were characterized by thermal analyses, ion-exchange capacities, streaming potentials, and pure water flux. Thermal analyses exhibited that the degradation temperature of the hybrid precursors decreased with an increase in zwitterionic extent because of the introduction of ion pairs. Ion-exchange capacity measurements revealed that the anion-exchange capacities and cation-exchange capacities were in the range of 0.023–0.05 and 0.32–0.58 mmol g⁻¹, respectively. Stream-

ing potentials displayed that when the membranes coated for one or three times, the isoelectric points were in the pH range of 6.6–7.58 and 6.58–7.7, respectively. The pure water flux showed that it could be affected by the coating times and the ingredients of these zwitterionic membranes. This difference in membrane's characteristics can be ascribed to the effect of molecular structure of the hybrid precursors. Both the Coulombic interactions of ion pairs between the polymer chains and the hydrophilicity of these membranes were proposed to clarify the above phenomena. © 2007 Wiley Periodicals, Inc. *J Appl Polym Sci* 105: 3162–3170, 2007

Key words: zwitterionic membrane; hybrid membrane; ion-exchange membrane; ion pairs; streaming potential

INTRODUCTION

With the rapid development of modern industries, environmental contamination has become increasingly severe in that numerous industrial wastes have ruthlessly polluted the natural environment, which was very suitable for the habitation of human being in the past. Meanwhile, the public attention for environmental protection is rapidly escalating, thus the treatment of industrial wastewater and the recovery of chemicals that will be wasted are becoming extremely important. With the drive to treat such environmentally harmful substances, innovative technologies to meet this demand have attracted many researchers. One of the promising technologies is the one based on ion-exchange membranes because it has such advantages as lower operation expense, secure process, and mature technology support.^{1,2} The researches for such membrane technology therefore are significantly im-

portant. In view of its significance, a great multitude of researchers thus have focused on this field since many years.^{3,4}

At present, various approaches have been proposed and developed to create inorganic–organic hybrid materials or membranes.^{5–7} Among them, the sol–gel process has become one of the most effective methods in that it provides a convenient, versatile, and low temperature-demanding route, and potential mixing of organic and inorganic components at the molecular level to produce hybrid systems, etc.^{6,8} Meanwhile, inorganic–organic hybrid charged materials or membranes, derived from such a sol–gel process, are becoming increasingly attractive because of the following reasons: the sol–gel route affords great simplicity^{8,9}; at the same time, the products prepared from such technique demonstrate advantageous properties, such as the structural flexibility, thermal and mechanical stability, etc.^{1,3,10} In particular, hybrid zwitterionic materials or membranes have been given especial attentions owing to their multifunctional group characteristics, and they expect to be applied in the separation of inorganic salts from water-soluble organic substances.¹¹ Up to now, many efforts have been made to explore hybrid zwitterionic materials.^{12–14} The investigation of hybrid zwitterionic membranes derived from such materials, however, is unsatisfactorily conducted so far.

Correspondence to: T. Xu (twxu@ustc.edu.cn).

Contract grant sponsor: Natural Science Foundation of China; contract grant number: 20576130.

Contract grant sponsor: National Basic Research Program of China; contract grant number: 2003CB615700.

Contract grant sponsor: Innovation Fund for the Graduate Students of USTC; contract grant number: KD2005022.

Journal of Applied Polymer Science, Vol. 105, 3162–3170 (2007)
© 2007 Wiley Periodicals, Inc.

TABLE I
Composition of Coating Solutions in the Alkoxide Solution System for the Hybrid Zwitterionic Membranes (Molar Ratio)

Membrane	TMSPEDA	APTMS	PAMTMS	TEOS	<i>n</i> -BuOH	1,4-Butyrolactone
A	0.1	—	—	0.1	0.4	0.5
B	—	0.1	—	0.1	0.4	0.5
C	—	—	0.1	0.1	0.4	0.5

Recently, in our laboratory, numerous efforts have been taken to synthesize and characterize hybrid charged membranes.^{15,16} With the motivation of developing novel ion-exchange membranes with antifouling feature, chemical stability, higher mechanical strength, and especially the higher permeability of electrolytes for purification of organic species,¹⁷ inorganic-organic hybrid zwitterionic materials and membranes have also been prepared and characterized in our laboratory.^{18–20} These zwitterionic membranes and materials have been synthesized successfully via a sol-gel process, followed by zwitterionization to create ion pairs on the polymer chains. Our continuing interest in such membranes stimulates us to further this research. Consequently, in this article, three types of novel hybrid zwitterionic membranes were synthesized by a coupling reaction between two silane-coupling agents and a subsequent reaction with 1,4-butyrolactone (BL) to produce ion pairs in the membrane precursors. Compared with those reported previously,^{18–20} particular attentions should be paid to the effect of molecular structure of hybrid precursors on the performances of these membranes.

EXPERIMENTAL

Materials

Phenylaminomethyl trimethoxysilane (PAMTMS) (>95.0%), *N*-[3-(trimethoxysilyl)propyl] ethylene diamine (TMSPEDA) (>95.0%), 3-aminopropyl trimethoxysilane (APTMS) (>95.0%), and tetraethoxysilane (TEOS) (>28.0%) were obtained from Silicone New Material Co. of Wuhan University (China) and used without further purification. 1,4-Butyrolactone (BL) (>97.0%), *n*-butanol (*n*-BuOH), and other reagents were of analytical grade; these chemicals were obtained from Shanghai Chemical Reagent Co. (China) and used as received. Microporous alumina plates were obtained commercially from ZiBo Ceramic Institute of Shandong (China), and had a symmetrical structure with 40–45% porosity, average pore diameter of near 1 μm, and total thickness of around 0.4 cm.

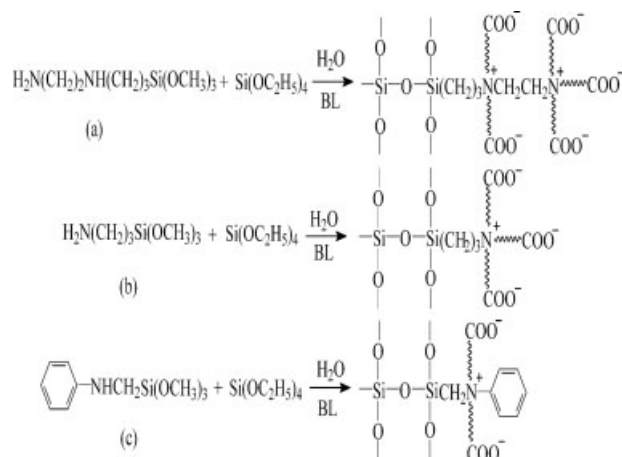
Preparation of the hybrid zwitterionic membranes

The membrane preparation procedure was as follows: the microporous alumina plate was immersed into different coating solutions whose chemical ingredients

were listed in Table I. After dip-coating for 15 min, the alumina plate was air-dried at room temperature for 30 min, kept at 60–70°C for 1 h and heat-cured at 110°C for additional 1 h, subsequently allowing it to cool off to the room temperature prior to obtaining the final membranes. This step might be repeated several times for the same alumina plate to increase the thickness of these investigated membranes.


To reduce the hydrolysis speed of the silicone, the sol-gel reaction was conducted in an *n*-BuOH solution system. The possible reactions for the hybrid zwitterionic membranes were presented in Scheme 1 and the structure unit of the membranes was dependent on the corresponding molecular structure of the used silane-coupling agents as listed in Table II. For each silane-coupling agent, the reactions included two steps: Step 1 was the hydrolysis and polycondensation reaction between the TMSPEDA, APTMS, or PAMTMS, respectively, and the TEOS, producing a hybrid precursor; Step 2 was a crosslinking reaction between the hybrid precursor and 1,4-butyrolactone. In Step 2, BL opened the lactone ring and reacted with the —NH₂— and/or —NH— groups in the hybrid precursor, leading to the creation of ion pairs grafted on the two sides of the polymer chain due to its amine structure.

Moreover, it should be noted that in the previous articles,^{18,19} the hybrid zwitterionic membranes and polymers were prepared by regulating the amount



Scheme 1 Possible reactions for the synthesis of hybrid zwitterionic membranes A–C were schematically illustrated in reaction formula (a–c), respectively.

TABLE II
Molecular Structure of the Silane-Coupling Agents Employed for the Preparation of the Hybrid Zwitterionic Membranes

Silane coupling agents	Chemical structure
<i>N</i> -[3-(trimethoxysilyl)propyl] ethylene diamine (TMSPEDA)	$\text{H}_2\text{NCH}_2\text{CH}_2\text{NH}(\text{CH}_2)_3\text{Si}(\text{OCH}_3)_3$
3-Aminopropyl trimethoxysilane (APTMS)	$\text{H}_2\text{NCH}_2\text{CH}_2\text{CH}_2\text{Si}(\text{OCH}_3)_3$
Phenylaminomethyl trimethoxysilane (PAMTMS)	
Tetraethoxysilane (TEOS)	$\text{Si}(\text{OC}_2\text{H}_5)_4$

of BL in the reaction process; whereas in this experiment, the hybrid zwitterionic membranes were synthesized from different structure units of hybrid precursors. The preparation technique in this case will be proved simpler and more practical than that used in the earlier work,^{18,19} this is because the selection of molecular structure of the membrane precursors is relatively easier than the quantity control of BL during the membrane preparation. Thus, it will provide a possibility to develop a hybrid zwitterionic membrane by properly selecting the chemical structure of the reagents.

Membrane characterizations

For determining the FTIR spectra of the samples from each step, the coating solution was smeared on the surface of NaCl salt plate, and then evaporated the *n*-BuOH under an ultraviolet lamp to form a stable film on the surface of such NaCl salt plate. The FTIR spectra of these samples can thus be recorded using a Bruker Equinox-55 FTIR spectrometer in the range of 4000–400 cm^{-1} with a resolution of 0.5 cm^{-1} .

To investigate the thermal stability of the membranes and appropriately select the heat-curing temperature during the membrane preparation, the thermal behavior (TGA and DrTGA) of the xerogels was determined by the thermogravimetric analysis (TGA-50H, Shimadzu Japan) in a nitrogen flow using a heating rate of 10°C min^{-1} . For the preparation of these xerogels, the coating solutions were dried at 70°C in a vacuum oven for 48 h to remove the *n*-BuOH, then allowing them to cool off to the room temperature. As a consequence, the white powders for the xerogels of the membranes A and B, respectively, and the yellow powder for the xerogel of the membrane C, could be obtained to qualify for the thermal analyses.

The anion-exchange capacities (AIECs) of the prepared hybrid zwitterionic membranes were determined by using the Mohr method, in which the membranes were converted to Cl^- form with an aqueous NaCl solution (0.1 mol dm^{-3}), and then back titrated with an aqueous AgNO_3 solution (0.01 mol dm^{-3}),

and the AIECs were expressed as mmol g^{-1} of dry-membrane.⁴ The cation-exchange capacities (CIECs) of the membranes were determined by using the similar method, in which the membranes were converted to Na^+ form with an aqueous NaOH solution (0.1 mol dm^{-3}), and subsequently back titrated with an aqueous HCl solution (0.01 mol dm^{-3}).^{19,20}

The measurement of streaming potentials ($\Delta E/\Delta P$) and the determination of isoelectric point (IEP) followed the same procedures as the earlier articles.^{1,20}

Pure water flux (*F*) of the explored membranes was conducted in a self-made dead-end membrane module.¹ The pressure difference used in this testing was around 0–2.5 MPa, and the effective membrane area was about 10.5 cm^2 . The total volume of water across the membranes was collected at a given time interval (1–10 min). To reduce the experimental errors, the mean values of thrice tests were selected as the final results. The uncertainties of water flux were estimated to be $\pm 5\%$. The water flux could be calculated as $F = V/(At\Delta P)$, where *V* stood for the total volume of the water permeated during the experiment. *A* represented the membrane area; *t* denoted the operation time; and ΔP was the pressure difference across the membranes.

RESULTS AND DISCUSSION

FTIR spectra

To demonstrate the reactions described in Scheme 1(a)–(c) and investigate the bonding coupling behaviors of the prepared products, FTIR spectroscopy was performed and the corresponding spectra were shown in Figure 1(a)–1(f).

As can be seen from Figures 1(a) and 1(b), the strong absorption peak at 1090 cm^{-1} was the overlapping bonds of Si–O–Si asymmetric stretching and Si–O–C stretching bands from trimethoxysilane groups of TMSPEDA and ethoxysilane of TEOS.²¹ The distinct absorption peaks associated with $-\text{CH}_3$ or $-\text{CH}_2-$ groups of *n*-BuOH and PAMTMS were observed at about 3000 cm^{-1} . The peak located at near 3300 cm^{-1} was ascribed to *N*–H bond, and the peak

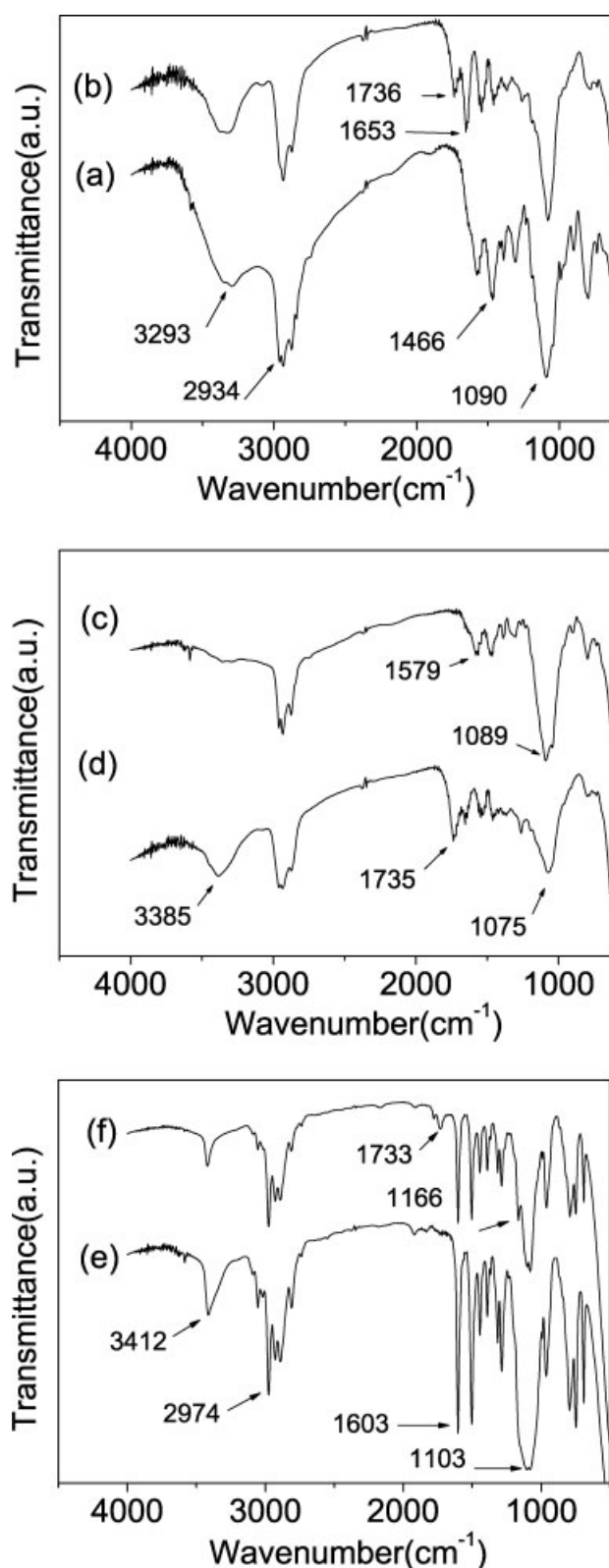


Figure 1 The FTIR spectra of: (a) the film of uncharged product of TMSPEDA reacted with TEOS; (b) the film corresponding to the membrane A; (c) the film of uncharged product of APTMS reacted with TEOS, (d) the film corresponding to the membrane B; (e) the film of uncharged product of PAMTMS reacted with TEOS, and (f) the film corresponding to the membrane C.

within the range of $1220\text{--}1500\text{ cm}^{-1}$ could be assigned to the C—N bond in the samples.^{19,22,23} After comparing Figure 1(b) with Figure 1(a), it can be found that the new peaks at 1550 and 1650 cm^{-1} were from the asymmetric stretching vibration of COO^- ,^{19,24} and the peak situated at 1735 cm^{-1} should be attributed to the C=O vibration, these changes in absorption peaks clearly confirmed the reactions described in Scheme 1(a), i.e., the occurrence of lactone-ring opening of BL and the formation of the zwitterionic polymer. In Figures 1(c) and 1(d), the FTIR spectra were similar in appearance except a little decrease in the intensity of concerned peaks to those observed in Figures 1(a) and 1(b), which confirmed the reactions illustrated in Scheme 1(b). In Figures 1(e) and 1(f), it should be noted that the sharp peak at 1604 cm^{-1} was attributed to the phenyl group in the samples,²⁰ and the other peaks were analogous to those observed in Figures 1(a)–1(d). The vibration of C=O group located at 1735 cm^{-1} [as depicted in Fig. 1(f)] corroborated the reactions presented in Scheme 1(c). In addition, it can also be found that within the range of $1780\text{--}1760\text{ cm}^{-1}$, no obvious evidence of the peak associated with the C=O vibration of lactone ring in BL was presented in the FTIR spectra of Figure 1(a)–1(f), implying the completion of the lactone-ring opening reaction of BL as presented in Scheme 1(a)–1(c), respectively.

Moreover, it should be emphasized that, after comparing the peak intensity of C=O groups associated with the carboxylic groups located at near 1735 cm^{-1} in Figures 1(b), 1(d), and 1(f), respectively, it can be found that these peaks' intensities follow the order: $B > A > C$. Such order suggested that the membrane B had the highest carboxylic groups content among membranes A–C, that is, the membrane B had the largest zwitterionic extent; whereas the membrane A, which possessed more active hydrogen than that of the membrane B, had a relatively lower one. This order was also proved by the IEC and streaming potential measurements (as shown in Figs. 4 and 5, hereinafter). These findings were beyond our expectation that the hybrid precursor containing more active hydrogen atoms in $\text{—NH}_2\text{—}$ and —NH— groups will graft more ion pairs on the chains of such zwitterionic polymers. It is hard to elucidate this phenomenon extensively within the authors' present knowledge; however, several ideas might be useful for explaining this unusual behavior.

Taking the membrane A into account, the chief reason why it does not exhibit the maximal content of ion pairs according to its molecular structure as presented in Scheme 1(a), is possibly related to both the reaction activity of $\text{—NH}_2\text{—}$ and —NH— groups in its hybrid precursor and the steric hindrance of the ion pairs grafted on the polymer chains. Namely, the primary amine is more active than the secondary one, while the steric hindrance derived from one ion

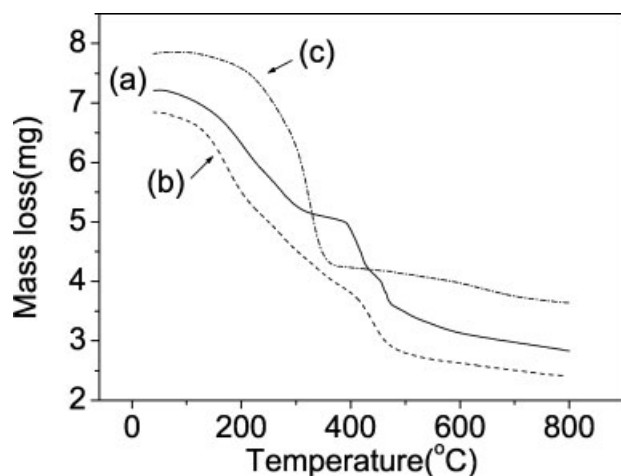


Figure 2 TGA curves of (a–c) for the hybrid precursor of the membranes A–C, respectively.

pair will inhibit another one's grafting, especially onto the neighboring nitrogen atom. In addition, the length of molecular chain will also conduce to this trend. It is well accepted that short chain of a polymer will favor the proceeding of the reaction between two molecules. Since the polymer chain of the hybrid precursor in the membrane B is shorter than that of in the membrane A, the reaction between the primary amine of the hybrid precursor in the membrane B with BL is perhaps easier than that of in the membrane A; the number of ion pairs in the membrane B is thus higher than that in the membrane A because of the combined effects of both the reaction activity of the amine groups and the steric hindrance of the ion pairs on the pendent side chains. Consequently, the peak intensity of C=O group at 1735 cm^{-1} in the membrane B is stronger than that in the membrane A as observed in Figures 1(a) and 1(b).

Furthermore, as concerns the molecular structure of the membrane precursors presented in Scheme 1(b) and 1(c), membranes B and C seem to have the same zwitterionic extent, but the above observation reveals that the amount of carboxylic groups in the membrane C is much lower than that in the membrane B; the cause might be due to the steric hindrance of phenyl group linked on the —NH— group in the hybrid precursor, which prevents the ion pairs from being grafted on such a —NH— group, leading to the lower content of ion pairs created in the polymer chain.

Thermal analysis

Understanding the degradation behavior and thermal stability of the organic groups are of vital importance in membrane preparation, thus both TGA and DrTGA analyses were conducted in a N_2 flow. The corresponding testing curves were illustrated in Figures 2 and 3.

It is interesting to find that, for different membranes A–C, the TGA curves (Fig. 2) clearly demonstrated different change trends in mass loss; meanwhile, corresponding to these mass loss stages, several endothermic peaks (mass loss peak) were exhibited in DrTGA curves (see Fig. 3). Moreover, it can be noted that, for the membrane A, three steps of mass loss are obvious. A sharp mass loss ($\sim 24\text{ wt}\%$) lower than 270°C was primarily caused by the evaporation and elimination of the solvent in the xerogel. A quick mass loss ($\sim 22\text{ wt}\%$) in the temperature range from 270 to 460°C could be ascribed to the decomposition of organic groups and the formation of silica. The steady mass loss (ca. $10\text{ wt}\%$) above 460°C was possibly due to the crystallization of silica. Regarding the membrane B, three steps of mass loss were discovered. A quick mass loss (ca. $32\text{ wt}\%$) below 280°C was the evaporation of solvent in the xerogel. The gradual mass loss (ca. $21\text{ wt}\%$) from 280 to 440°C was chiefly caused by the decomposition of organic groups and the formation of silica. The steady mass loss (ca. $9\text{ wt}\%$) above 440°C was probably due to the crystallization of silica. However, unlike those detected in the TGA curves of the membranes A and B, only a one-step mass loss was observed in that of the membrane C. The mass loss (ca. $45\text{ wt}\%$) less than 325°C was largely brought by the evaporation and elimination of solvent in the xerogel as well as the gradually degraded phenyl groups in the sample. The slight mass loss (ca. $8\text{ wt}\%$) above 325°C could be assigned to the crystallization of silica.

Figure 3 is the DrTGA curves of membranes A–C. As presented in Figures 3(a)–3(c), there existed different endothermic peaks in the DrTGA curves, which indicated different thermal degradation behaviors as revealed in TGA curves (cf. Fig. 2). In addition, the temperature of the first mass loss peak, which repre-

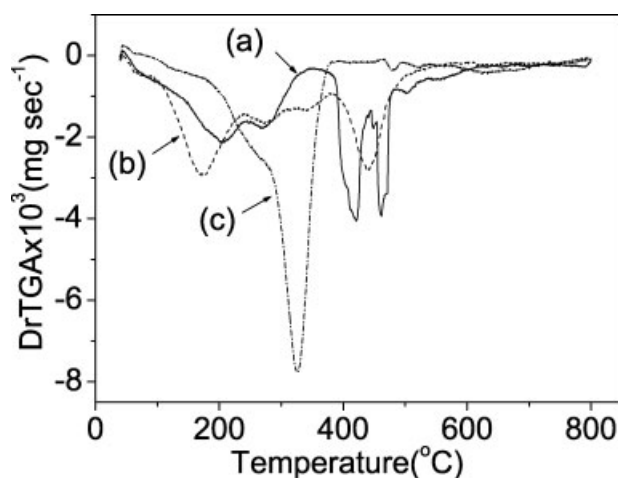


Figure 3 DrTGA curves of (a–c) for the prepared membranes A–C, respectively.

sented the beginning of the thermal decomposition, was 325, 204, and 170°C for membranes C, A, and B, respectively, implying a decline trend in the thermal degradation temperature with an increase in the zwitterionic extent of the synthesized membranes. Such result was consistent with the observations in FTIR spectra as shown in Figure 1. The above phenomena in thermal behaviors clearly showed the effect of molecular structure of hybrid precursors on the membrane's features.

Furthermore, to have an insight into such trend, special attention should be given to the significant difference in the zwitterionic extent of the investigated membranes. It is well known that the higher the organic composition in a substance, the lower its thermal degradation temperature will be. Since the organic ingredients in the membranes enhanced with the increasing content of ion pairs grafted on the polymer chains, the degradation temperature of this hybrid precursor should decrease accordingly. Consequently, the degradation temperature of the membrane B lower than that of membrane A was mainly due to its higher ion pair content as mentioned in FTIR spectra. As for the abnormal phenomenon observed in the membrane C, its higher degradation temperature was primarily assigned to the existence of phenyl groups in the hybrid precursor, which was apparently hard to be decomposed among the organic groups.

Determination of ion-exchange capacity

To further verify the reactions described in Scheme 1 and probe the electrical properties of the tested membranes, the ion-exchange capacities (IECs) for both anionic and cationic groups were determined and the measured results were illustrated in Figures 4(a) and 4(b).

It can be noted that the anion exchange capacities (AIECs) of the three types of hybrid zwitterionic mem-

branes were in the range of 0.023–0.05 mmol g⁻¹, suggesting that the membranes possessed anion exchange groups. Meanwhile, the cation exchange capacities (CIECs) of these membranes were in the range of 0.32–0.58 mmol g⁻¹, implying that they also contained cation exchange groups. These outcomes demonstrate that the above-developed membranes can exhibit the features of both positively and negatively charged groups, which further corroborates the reaction depicted in Scheme 1, i.e., the lactone-ring opening of BL and the zwitterionic reaction have occurred during the membrane preparation.

Moreover, it can be found in Figures 4(a) and 4(b) that both the AIECs and CIECs were affected greatly by the composition of the hybrid precursors and the coating times. For example, for the same ingredients of the membranes A–C, both the AIECs and CIECs enhanced with an increase in coating times. The theoretical explanation of these trends is that both the positively and negatively charged groups increase with the rising coating times due to an increase in the deposited materials on the membrane surface, resulting in the promotion of ion-exchange ability. Whereas for the same coating times of the membranes originated from different hybrid precursors, both the AIECs and CIECs displayed the same change trends: the membrane B had the highest IECs among them. These results in the IECs also follow the order of zwitterionic extent as observed in FTIR spectra (cf. Fig. 1). This tendency can be ascribed to the distinction in the zwitterionic extent of the investigated membranes. In general, IEC is the reflection of ion-exchange ability of a membrane, which is primarily related to the quantity of anions or cations in the membrane. In this case, the membrane B has the highest content of carboxylic groups among membranes A–C, whereas the membrane C has the lowest one; therefore the IECs follow the same order as above.

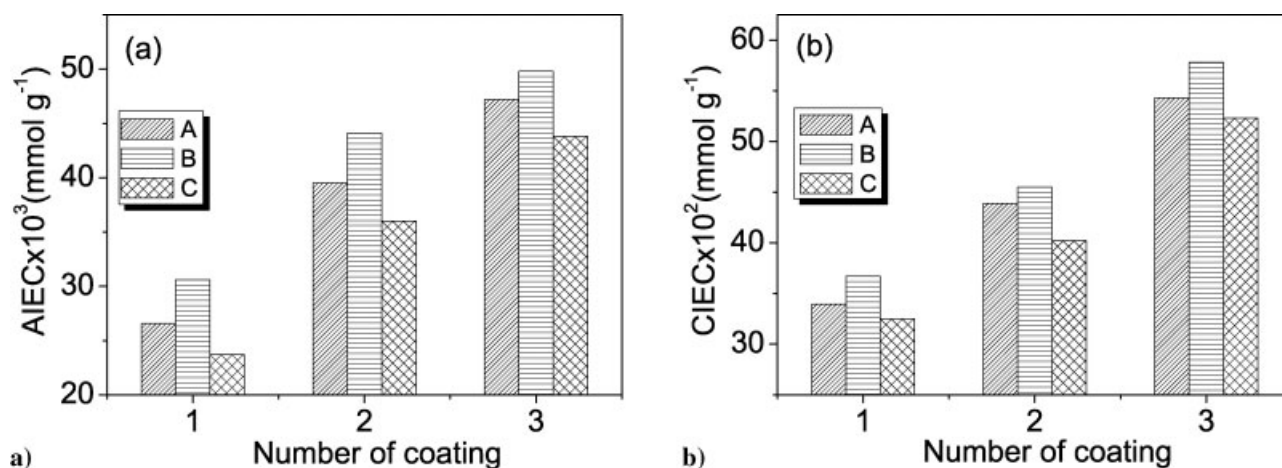


Figure 4 The influence of coating times on both the AIECs (a) and CIECs (b) of the membranes.

Furthermore, it should be pointed out that in view of the structure of the produced membranes [Scheme 1(a)–1(c)], the molar number of anionic groups is about 2–3 times larger than that of cationic groups. However, from the experimental data of IECs, the CIECs of the membranes are nearly 10 times higher than the AIECs (Figs. 4(a) and 4(b)). Several major factors might be responsible for this tendency. One is associated with the residual BL in the membranes, which can be easily transferred to butyric acid (BA) and favors the increase in the CIECs during the membrane preparation, resulting in a great difference between the IECs of cationic and anionic groups as discussed in a previous article.²⁰ Another can be assigned to the molecular structure of the hybrid precursors. On the one hand, the negatively charged groups are located on the pendent side chains or situated on the chain terminals of the polymer backbones [Scheme 1(a)–1(c)], which possibly tend to contribute positively to the ion-exchange capacity. On the other hand, the positively charged groups are positioned on the main chains of the polymers [cf. Scheme 1(a)–1(c)], and it is difficult for them to conduct ion exchange because of both the steric hindrance and the charge-charge repulsion of the quaternary ammonium groups.²⁵ In addition, the IEC difference might also be caused by either the low positive charge density on the membrane matrix or low extent of dissociation of anion-exchange functional groups under the measuring conditions. As a result, they also give rise to some contributions to the great difference between the CIECs and AIECs.

Streaming potentials and IEP

It is reported that the membrane containing both positively and negatively charged groups has an IEP.⁴ In this case, the prepared hybrid zwitterionic

membranes also possessed ion pairs as depicted in Scheme 1, therefore, it is supposed to exist an IEP in these membranes and this IEP could be determined by the measurement of streaming potentials.²⁰ The streaming potentials were thus measured and the results were shown in Figures 5(a) and 5(b).

It can be seen that the streaming potentials of the explored membranes were affected by both the coating times and the chemical structure of the hybrid precursors. As observed in Figures 5(a) and 5(b), no matter whether the membranes were coated one or three times, the IEPs exhibited an upward trend with the increasing content of ion pairs in the membranes. These IEPs were in the pH range of 6.6–7.58 for the membranes coated one time (pH 6.6, 7.3, and 7.58 for the membranes C, A, and B, respectively), and pH 6.58–7.7 for the membranes coated thrice (pH 6.58, 7.56, and 7.7 for the membranes C, A, and B, respectively), indicating an increasing trend with the growing zwitterionic extent. In addition, taking these IEPs into consideration, it can be discovered that there existed a good agreement among them if neglecting the experimental errors.

Moreover, although the above IEPs displayed a similar rising tendency, the streaming potentials against pH values presented different change trends. For instance, when the membranes A–C were coated one time, the streaming potentials against pH values exhibited an upward trend, i.e., they increased from negative to positive values as pH increases [see Fig. 5(a)]. Whereas, when these membranes were coated thrice, the streaming potentials vs. pH values changed from positive to negative values with pH elevating [cf. Fig. 5(b)]. These distinctions in streaming potentials clearly reveal the influence of coating times and the molecular structure of the hybrid precursors on the performances of the investigated membranes.

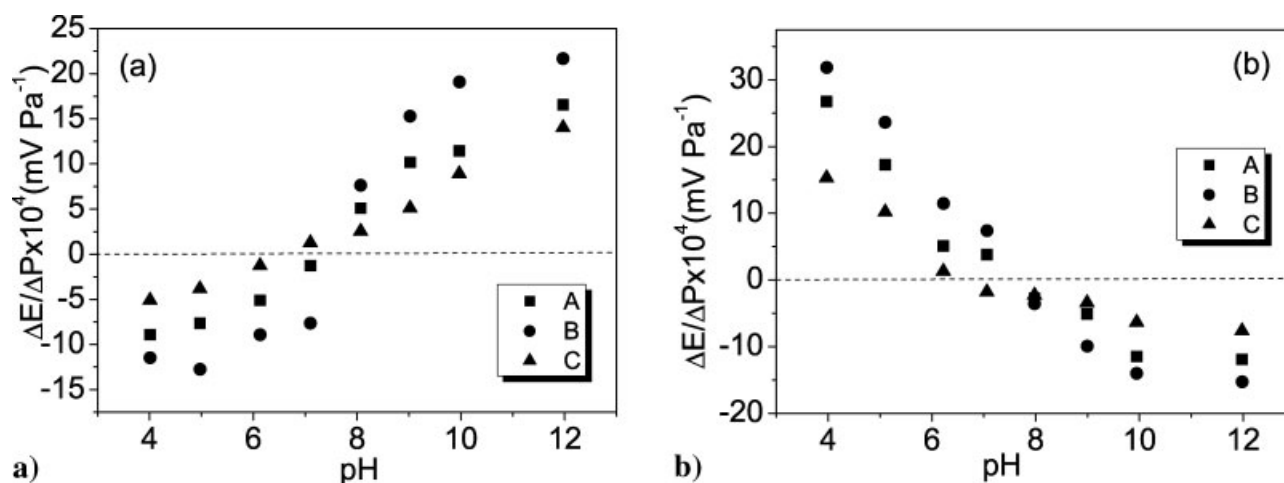


Figure 5 Streaming potentials of the prepared membranes coated: (a) one time, (b) thrice. A–C correspond to the membranes listed in Table I.

To give an explanation to the above phenomena, special attentions should be paid to the surface charge of these membranes and the possible adsorption behavior of the ions, which changed with the pH value of the external solution as discussed earlier.¹⁹ If the membranes were coated one time [cf. Fig. 5(a)], the amount of both anionic and cationic charge sites was relatively small and the mobile ions in the external solution might form a single ionic adsorption layer on the membrane surface. Accordingly, the membranes displayed positive charge properties when the pH value was lower than the IEP (in the acidic condition) in that the carboxylic groups were protonated,²⁵ and they displayed negative charge properties when the pH value was higher than the IEP (in the basic condition).¹⁹ However, when the membranes were coated thrice [see Fig. 5(b)], the quantity of the anionic charge sites was higher than that of the cationic ones because of an increase in carboxyl groups in the membrane precursors (see Scheme 1), thus the electrolyte solution might easily produce multi-ionic adsorption layers on membrane surface, while the acidity of amine groups was quite weaker than that of the carboxylic groups in these membranes. As a result, the properties of cationic groups were weaker than those of anionic groups in the prepared membranes. Consequently, the streaming potentials against pH values indicate different change trends.

Measurements of pure water flux

To examine the effect of the hybrid precursors on the performances of these prepared membranes A–C, pure water flux was conducted and the results were summarized in Table III.

It is quite interesting to find that both the membrane ingredients and the coating times can highly affect the pure water flux of the membranes. For example, for the same composition of the membranes, pure water flux decreased considerably with an increase in coating times. The main reason of this tendency might be related to an increase in membrane thickness with the increasing coating times, which resulted in the shrinkage of the membrane pore size.^{1,20} However, for the same coating time of

the membranes with different ingredients (Table I), water flux displayed diverse change trends, which was dependent on the content of ion pairs in the membranes, i.e., pure water flux decreased with the order of membranes A > C > B. This trend can be explained theoretically by the Coulombic interactions between ion pairs and the difference between molecular structures of the hybrid precursors (see Table II). After the introduction of ion pairs onto the main chains of the hybrid precursors, the impact of Coulombic attractions between anionic and cationic groups²⁶ will increase with the increasing zwitterionic extent, the tightness of the membranes thus increases,^{26,27} leading to the shrinkage of membrane pore size and the subsequent fall in water flux. For instance, as stated in FTIR spectra (Fig. 1, hereinbefore), the number of ion pairs in the prepared membranes A–C followed the order: B > A > C, i.e., the membrane B had the largest zwitterionic extent among these membranes. Its water flux as observed in Table III, however, presented the minimum among them, indicating a completely different change trend between the water flux and zwitterionic extent. Therefore, it can be deduced from the above experience that the drop in water flux could be ascribed to the combined effects of the Coulombic interactions between ion pairs and the shrinkage of membrane pore size.

Moreover, it should be noted that according to the Coulombic attractions between ion pairs, the water flux of the membrane A should be lower than that of membrane C, but the actual trend in water flux is apparently opposite to this deduction. It is difficult to explain this phenomenon extensively; however, the hydrophilicity of the membranes might be responsible for this abnormal behavior. As mentioned above, the number of carboxylic groups in the membrane A was higher than that of the membrane C. These carboxylic groups are capable of increasing the hydrophilicity of the hybrid zwitterionic membranes in that they conduce to the penetration of water molecules; meanwhile the hydrophilicity enhances with the increasing content of the carboxylic groups in the membranes as reported previously,^{19,20,25} the water flux thus increase accordingly. What's more, the phenyl group in the membrane C is a hydrophobic group, which will result in a decrease in the hydrophilicity of such membrane. The water flux across the membrane C is, therefore, lower than that of the membrane A. Consequently, it can be concluded that hydrophilicity is one of the major impact factors on the water flux of the tested membranes.

CONCLUSIONS

A series of novel hybrid zwitterionic membranes have been synthesized through a coupling reaction

TABLE III
Pure Water Flux [$\text{l (m}^2 \text{ Pa h)}^{-1}$] of the Membranes
A–C Coated for Different Times

Coating times	Membrane A (10^{-4})	Membrane B (10^{-4})	Membrane C (10^{-4})
Without coating	650	728	685.5
1	501.2	9.6	120
2	410.6	5.74	75.7
3	335	3.81	46.9
4	216.8	1.53	31.1

between two silane-coupling agents in the alcohol solution system, and a subsequent reaction with BL to produce ion pairs in the membrane precursors. The degradation temperature of these hybrid precursors decreased with an increase in the zwitterionic extent. This declining trend in thermal degradation temperature could be ascribed to the introduction of ion pairs to the polymer chains. The IECs demonstrated that the AIECs of the membranes were in the range of 0.023–0.05 mmol g⁻¹; and the CIECs ranged from 0.32 to 0.58 mmol g⁻¹, which was also related to the zwitterionic extent of the produced hybrid precursors. Streaming potentials revealed that when the membranes were coated for one or three times, the IEPs were in the pH range of 6.6–7.58 and 6.58–7.7, respectively, and these IEPs enhanced with the increasing zwitterionic extent. The pure water flux showed that it could be affected by the coating times and the compositions of the prepared membranes. Both the Coulombic interactions between charged groups and the membrane's hydrophilicity were put forward to explain the above change trends in the membrane's properties. These findings suggested that the molecular structure of the hybrid precursors could dominate the performances of these investigated membranes.

References

1. Wu, C. M.; Xu, T. W.; Yang, W. H. *J Membr Sci* 2003, 224, 117.
2. Komkova, E. N.; Stamatialis, D. F.; Strathmann, H.; Wessling, M. *J Membr Sci* 2004, 244, 25.
3. Villamo, O.; Barboiu, C.; Barboiu, M.; Yau-Chun-Wan, W.; Hovnanian, N. *J Membr Sci* 2002, 204, 97.
4. Nonaka, T.; Matsumura, S.; Ogata, T.; Kurihara, S. *J Membr Sci* 2003, 212, 39.
5. Kulkarni, S. S.; Kittur, A. A.; Aralaguppi, M. I.; Kariduraganavar, M. Y. *J Appl Polym Sci* 2004, 94, 1304.
6. Bandyopadhyay, A.; Sarkar, M. D.; Bhowmick, A. K. *J Appl Polym Sci* 2005, 95, 1418.
7. Sawada, H.; Yoshioka, H.; Kawase, T.; Takahashi, H.; Abe, A.; Ohashi, R. *J Appl Polym Sci* 2005, 98, 169.
8. Adeogun, M. J.; Hay, J. N. *J Sol-Gel Sci Tech* 2001, 20, 119.
9. Chen, W.; Feng, H.; He, D.; Ye, C. *J Appl Polym Sci* 2004, 67, 139.
10. Nagarale, R. K.; Shahi, V. K.; Rangarajan, R. *J Membr Sci* 2005, 248, 37.
11. Baker, R. W. *Membrane Technology and Applications*, 2nd ed.; Wiley: Chichester, 2004.
12. Favresse, P.; Laschewsky, A.; Emmermann, C.; Gros, L.; Linsner, A. *Eur Polym J* 2001, 37, 877.
13. Innocenzi, P.; Miorin, E.; Brusatin, G.; Abbotto, A.; Beverina, L.; Pagani, G. A.; Casalboni, M.; Sarcinelli, F.; Pizzoferrato, R. *Chem Mater* 2002, 14, 3758.
14. Litt, M.; Matsuda, T. *J Appl Polym Sci* 1975, 19, 1221.
15. Wu, C. M.; Xu, T. W.; Gong, M.; Yang, W. H. *J Membr Sci* 2004, 247, 111.
16. Liu, J. S.; Xu, T. W.; Gong, M.; Fu, Y. X. *J Membr Sci* 2003, 264, 87.
17. Itou, H.; Toda, M.; Ohkoshi, K.; Iwata, M.; Fujimoto, T.; Miyaki, Y.; Kataoka, T. *Ind Eng Chem Res* 1988, 27, 983.
18. Liu, J. S.; Xu, T. W.; Fu, Y. X. *J Non-Cryst Solids* 2005, 351, 3050.
19. Liu, J. S.; Xu, T. W.; Fu, Y. X. *J Membr Sci* 2005, 252, 165.
20. Liu, J. S.; Xu, T. W.; Gong, M.; Fu, Y. X. *J Membr Sci* 2005, 260, 26.
21. Innocenzi, P.; Brusatin, G.; Guglielmi, M.; Bertani, R. *Chem Mater* 1999, 11, 1672.
22. Matsuura, Y.; Miura, S.; Naito, H.; Inove, H.; Matsukawa, K. *J Organomet Chem* 2003, 685, 230.
23. Jung, M. *Int J Inorg Mater* 2001, 3, 471.
24. Ayora-Cañada, M. J.; Lendl, B. *Vib Spectrosc* 2000, 24, 297.
25. Kathmann, E. E.; McCormick, C. L. *J Polym Sci Part A: Polym Chem* 1997, 35, 243.
26. Lowe, A. B.; McCormick, C. L.; *Chem Rev* 2002, 102, 4177.
27. Nagarale, R. K.; Gohil, G. S.; Shahi, V. K.; Rangarajan, R. *Macromolecules* 2004, 37, 10023.